AD-A059 727 CIVIL ENGINEERING LAB (NAVY) PORT HUFNEME CALIF F/G 13/10
THE BEHAVIOR OF AN INCLINED PONTOON BREAKWATER IN WATER WAVES.(U)
MAY 78 F RAICHLEN, J LEE

UNCLASSIFIED NL

1 OF 1
AD A059727

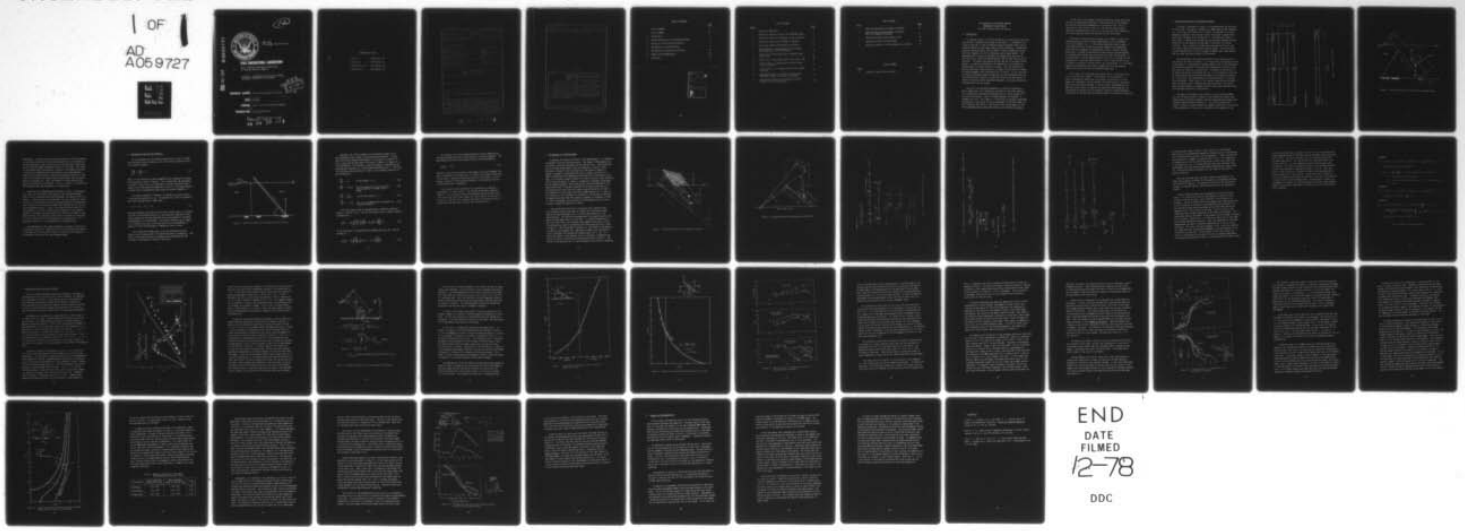

END
DATE FILMED
12-78
DDC

PO NO. N62583/78 M R552

CIVIL ENGINEERING LABORATORY

NAVAL CONSTRUCTION BATTALION CENTER
Port Hueneme, California 93043

TITLE: THE BEHAVIOR OF AN INCLINED PONTOON BREAKWATER IN WATER WAVES

CORPORATE AUTHOR: Fredric Raichlen and Jiin-jen Lee

DATE: May 1978

SPONSOR: Naval Facilities Engineering Command

PROGRAM NOS. YF53 536 091 01.002A

approved for public release
distribution unlimited.

CONVERSION OF UNITS

1 foot (ft)	=	0.3048 meter (m)
1 inch (in.)	=	0.0254 meter (m)
1 pound force (lb)	=	4.448 Newtons (N)
1 ton force (T)	=	8896 Newtons (N)

Unclassified

SECURITY CLASSIFICATION OF THIS PAGE (When Data Entered)

REPORT DOCUMENTATION PAGE		READ INSTRUCTIONS BEFORE COMPLETING FORM
1. REPORT NUMBER PO No. N62583/78 M R552	2. GOVT ACCESSION NO. AD-A787093	3. RECIPIENT'S CATALOG NUMBER
4. TITLE (and Subtitle) THE BEHAVIOR OF AN INCLINED PONTOON BREAKWATER IN WATER WAVES		5. TYPE OF REPORT & PERIOD COVERED Not final; Nov 1976 – Apr 1978 6. PERFORMING ORG. REPORT NUMBER
7. AUTHOR(s) Fredric Raichlen and Jiin-jen Lee		8. CONTRACT OR GRANT NUMBER(s)
9. PERFORMING ORGANIZATION NAME AND ADDRESS Dr. Fredric Raichlen Pasadena, California 91109		10. PROGRAM ELEMENT, PROJECT, TASK AREA & WORK UNIT NUMBERS 62760N; YF53.536.091.01.002A
11. CONTROLLING OFFICE NAME AND ADDRESS CIVIL ENGINEERING LABORATORY Naval Construction Battalion Center Port Hueneme, California 93043		12. REPORT DATE May 1978 13. NUMBER OF PAGES 43
14. MONITORING AGENCY NAME & ADDRESS(if different from Controlling Office) Naval Facilities Engineering Command Alexandria, Virginia 22332		15. SECURITY CLASS. (of this report) Unclassified 15a. DECLASSIFICATION/DOWNGRADING SCHEDULE

16. DISTRIBUTION STATEMENT (of this Report)

Approved for public release
distribution unlimited

17. DISTRIBUTION STATEMENT (of the abstract entered in Block 20, if different from Report)

18. SUPPLEMENTARY NOTES

19. KEY WORDS (Continue on reverse side if necessary and identify by block number)

Floating breakwaters; wave transmission; mooring force; analytical model; experiments.

20. ABSTRACT (Continue on reverse side if necessary and identify by block number)

The inclined pontoon breakwater, or sloping float breakwater, is a row of bargelike pontoons moored so that, at rest, the shoreward ends, which are ballasted, rest on the seafloor while the seaward ends, which are buoyant, project slightly above the water surface.

The development of a prediction technique for wave attenuation, motion, and mooring forces was initiated with the formulation of an analytical model. Experiments in a wave tank with a hinged plate were conducted, and the results confirm (continued)

DD FORM 1 JAN 73 1473 EDITION OF 1 NOV 65 IS OBSOLETE

Unclassified

SECURITY CLASSIFICATION OF THIS PAGE (When Data Entered)

20. Continued

certain elements of the mathematical model. Data on wave transmission and mooring forces were obtained from initial experiments with a model barge (pontoon).

Library Card

Civil Engineering Laboratory
THE BEHAVIOR OF AN INCLINED PONTOON BREAKWATER IN WATER WAVES, by Fredric Raichlen and Jiin-jen Lee
PO No. N6258378MR55243 pp illus/May 1978/Unclassified

1. Floating breakwater 2. Analysis I. YF53.536.091.01.002A

The inclined pontoon breakwater, or sloping float breakwater, is a row of bargelike pontoons moored so that, at rest, the shoreward ends, which are ballasted, rest on the seafloor while the seaward ends, which are buoyant, project slightly above the water surface.

The development of a prediction technique for wave attenuation, motion, and mooring forces was initiated with the formulation of an analytical model. Experiments in a wave tank with a hinged plate were conducted, and the results confirm certain elements of the mathematical model. Data on wave transmission and mooring forces were obtained from initial experiments with a model barge (pontoon).

TABLE OF CONTENTS

		Page
	LIST OF FIGURES	ii
	LIST OF PLATES	iii
1.	Introduction	1
2.	General Description of the Analytical Model	3
3.	Evaluation of the Velocity Potential	7
4.	The Dynamics of the Moored Body	11
5.	Presentation and Discussion of Results	20
6.	Summary and Recommendations	40
7.	References	43

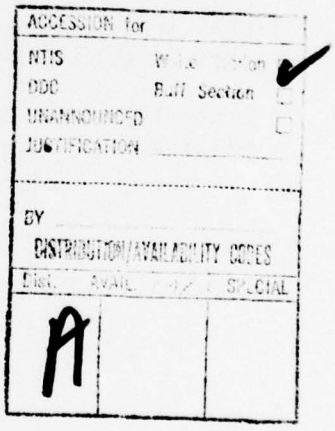

LIST OF FIGURES

Figure		Page
1	Drawing of AMMI barge	4
2	Definition sketch for moored semi-submerged barge	5
3	Definition sketch for evaluation of wave potential	8
4	Definition sketch for the change in buoyancy	12
5	Definition sketch for mooring line restraint	13
6	Wave generation characteristics of an inclined-plate generator; α = 21.8° and 90°	21
7	Deflection of board with elastic restraint under static load	25
8	Deflection of unrestrained plate under static load	26
9	Characteristics of hinged plate with and without elastic restraint	27
10	Characteristics of a hinged plate with and without clearance	31
11	Equilibrium angle for an unmoored, partly sunk AMMI barge; center of gravity at mid-length	34
12	Transmission coefficient and maximum developed mooring force for moored barge	38

LIST OF PLATES

Plate		Page
1	Equations Describing the Change in Buoyancy	14
2	Equations Describing the Moment Introduced Due to the Change in Buoyancy	15
3	The Restoring Force for an Elastic Line	16
4	Equations of Motion of Moored Body	19
5	Equation of Motion of a Plate Hinged at the Bottom	23

LIST OF TABLES

Table		Page
1	Moment of Inertia per Unit Width	35

THE BEHAVIOR OF AN INCLINED PONTOON BREAKWATER IN WATER WAVES

by Fredric Raichlen and Jiin-jen Lee

1. Introduction

An important aspect of offshore operations is the ability to continue these during a reasonably wide range of sea-states. To accomplish this it may be desirable to have available portable breakwaters which can be deployed rapidly and used under widely varying conditions. A method was proposed some years ago by Patrick (1951) in which an amphibious breakwater was suggested for use in relatively shallow water depths. The breakwater was to consist of pontoons (or barges) which were sunk so that the bow (or stern) touched the bottom, and the other end was out of the water. The pontoon was moored with the end out of the water facing seaward. A study was conducted in the laboratory to investigate the characteristics of these structures in waves. The wave transmission features and certain observations of the details of the motion of models of these breakwaters were reported by Patrick (1951). It was found that this mobile breakwater might be promising, but the experiments were too simplified and not conducted in sufficient scope to use the results to predict the mooring forces and detailed aspects of the wave transmission characteristics of such systems.

The use of such portable breakwaters is attractive compared to other schemes due to its simplicity, availability, and other features, but, as mentioned, the detailed characteristics of these systems still are relatively unknown. Thus, for design purposes the engineer is somewhat at a loss. This report is a first step in trying to understand the dynamics of the motion of such a breakwater in sufficient detail so that ultimately the forces in the mooring lines and the motion of the semi-submerged pontoons under wave action can be determined a priori.

At the crux of the problem of predicting mooring forces associated with an inclined-pontoon breakwater is the evaluation of the pressure distribution around the breakwater as a function of time. This is necessary for the solution, since it is the forcing function which causes the breakwater motion and, hence, provides the input from which the transmitted wave height and mooring force are determined.

The overall problem has been divided into a number of steps to be treated analytically and confirmed experimentally as work proceeds. These "sub-problems" are: an inclined wave generator where a plate is oscillated with known stroke and the waves generated are determined analytically and compared to experimental results; a partly floating plate which is hinged at the bottom with and without a gap and exposed to incident waves without any restraining force other than buoyancy; an accurate model of the prototype barge which consists of a barge inclined and moored in a nonlinear fashion which is free to move off the bottom. To obtain an analytical solution to the last "sub-problem" it is considered necessary and important to be able to handle the first two problems analytically with the results confirmed by experiments.

This report will be divided into several parts: an overall discussion of the analytical model, a discussion of the wave potential in regions upstream and downstream of the barge, a discussion of various aspects of the dynamics of the problem, and a description of the experiments which have been conducted. Finally, certain recommendations are made for future studies to complete the analytical model begun here so that design information can be provided to determine optimum breakwater characteristics and moorings for expected ranges of coastal wave conditions.

2. General Description of the Analytical Model

A drawing is presented in Figure 1 of the barge which was the basis for this study. The barge is denoted as an AMMI barge and the dimensions are: 90 ft long, 28 ft wide, and 5 ft deep. The concept is to partly submerge the barge so that one end sinks to the bottom in depths which could vary from about 20 ft to about 50 ft. The other end, which is above water, is moored with the mooring line extending seaward such that the portion of the barge out of the water is pointing in a seaward direction. Thus, a normally incident wave from the open sea will see this barge as making an acute angle with the bottom. (Future work may indicate possibilities of similar systems in deeper water, even moored with the lower end some distance off the bottom.)

The orientation of the barge and certain of the notation used in the analysis are shown in Figure 2. For waves which are normally incident to the barge it is reasonable to develop a model which is two-dimensional, and the possible motions of the barge when referenced to the axis shown are surge (x), heave (y), and pitch (ψ). The object of the analysis is to predict the tension of the mooring line, T, as a function of time due to incident waves and to determine the motion of the center of gravity as a function of time (and the motion of the point which is in contact with the bottom). (This latter is of interest since the earlier experiments of Patrick (1951) indicated that the point which is in contact with the bottom moved in a seaward direction under some conditions which would decrease the mooring line tension.)

The general philosophy of the solution is to divide the problem into the two regions shown in Figure 2, the incident wave region (the seaward region) defined as Region I and the transmitted wave region (the shoreward region) defined as Region II. The velocity potential is sought in these two regions subject to boundary conditions on the surface of the barge which, of course, are a function of the dynamics of the

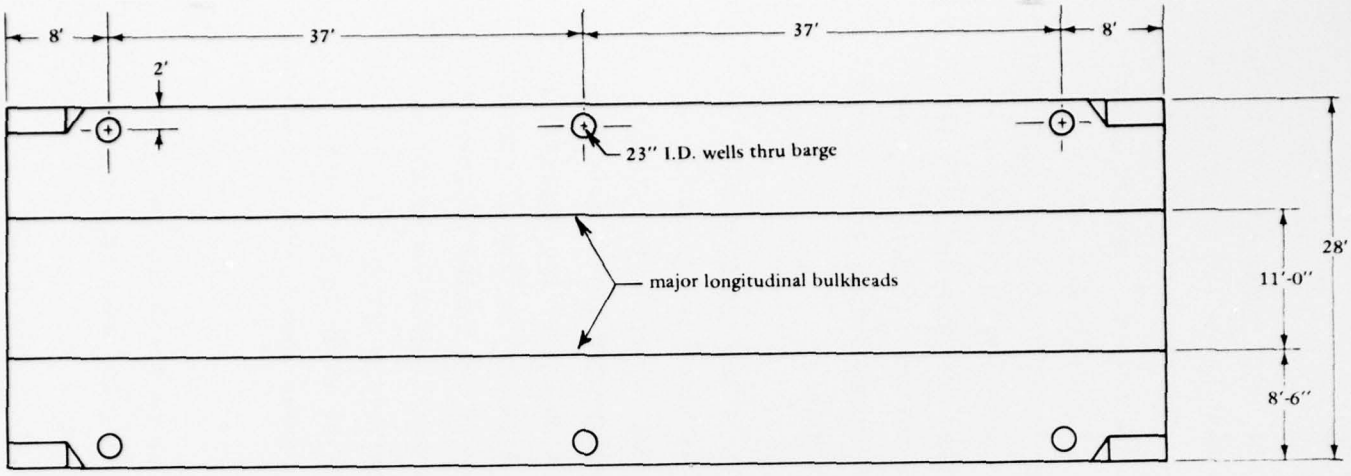

PLAN

Approximate Weight, 50 tons

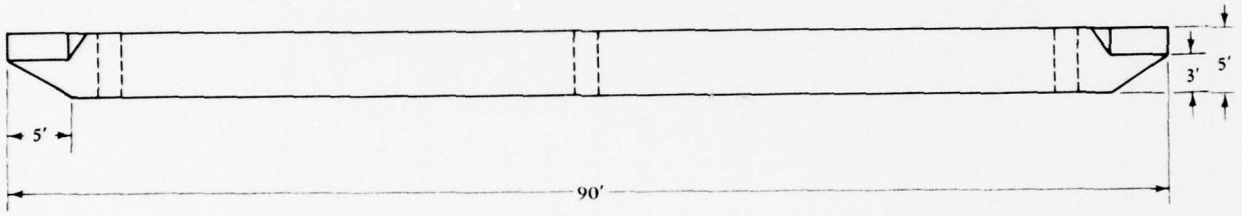

ELEVATION

Figure 1. Drawing of AMMI barge.

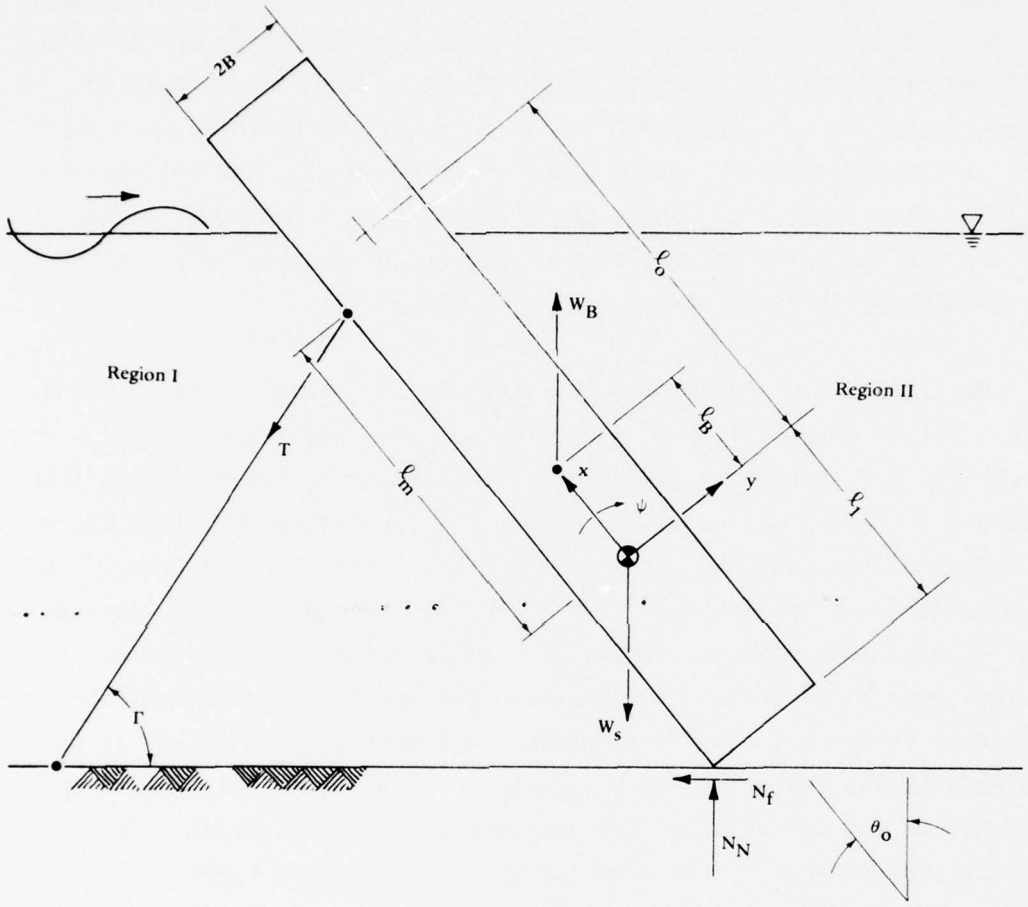

Figure 2. Definition sketch for moored semi-submerged barge.

moored body. In other words, the velocity potentials are to be matched so the normal derivative of the velocity potentials at the surface of the moored barge are equal at each point to the velocity of that point derived from the dynamic equations of motion of the barge. This leads to the approach where the equations of motion of the barge are written in terms of an unknown pressure distribution on the body defined in terms of the time derivative of the velocity potential which is a function of the incident wave height, period, water depth, and inclination angle of the barge, etc. Thus, the problem is complicated with the motions and the waves interrelated. This is, of course, very similar to the problem of defining the motions of a moored ship.

Physically the problem may be described as follows: the incoming wave causes an oscillation of the barge in some complicated manner which, in turn, generates waves which propagate into Region II and into Region I. The objectives are to determine, for various physical characteristics of the body and its mooring, the amplitude of the transmitted wave relative to the incident wave amplitude, the mooring line tension, and the attendant motions. There is one simplified model which can be investigated in an effort to understand the dynamics of the complete problem. This model considers the body not moored but "hinged" at the bottom with the restoring force associated with the motion of the body due only to the variation of the buoyancy as the barge moves. The equations of motion for this problem will be presented later.

The development of the velocity potential in Regions I and II will be outlined in Section 3. Where this fits into the equations of motion of the body will be discussed in Section 4 along with other aspects of the dynamics of motion of the semi-submerged barge.

3. Evaluation of the Velocity Potential

For the evaluation of the velocity potential the fluid is assumed inviscid and the flow irrotational; thus, the velocity potential satisfies Laplace's equation:

$$\frac{\partial^2\phi}{\partial x^2} + \frac{\partial^2\phi}{\partial y^2} = 0 \tag{1}$$

where x is the direction of wave propagation and y represents the depthwise direction as shown in Figure 3. (It is noted that the coordinates x,y used in Figure 3 are, for simplicity, different from those used in Figure 2 and in developing the equations of motion of the barge; however, a simple linear transformation makes these two systems indentical.)

The velocity potential in Region I is denoted as ϕ_I and in Region II the velocity potential is ϕ_{II}. The potential ϕ_I can be considered as the linear superposition of three parts:

$$\phi_I = \phi_i + \phi_r + \phi_s \tag{2}$$

where ϕ_i represents the potential due to the incident wave, ϕ_r represents that due to the reflected wave (as if the barge were completely fixed) and ϕ_s denotes the velocity potential due to the movement of the barge represented as an inclined plate. The velocity potential ϕ_{II} in Region II is related to ϕ_s only, since there would be no wave generated in Region II if the inclined barge is completely fixed in place.

For a specified incident wave, ϕ_r can be evaluated relatively easily; thus, the major part of the effort has been to evaluate ϕ_s. The motion of the plate upon which ϕ_s depends must be matched with the solution of the equation of motion of the plate.

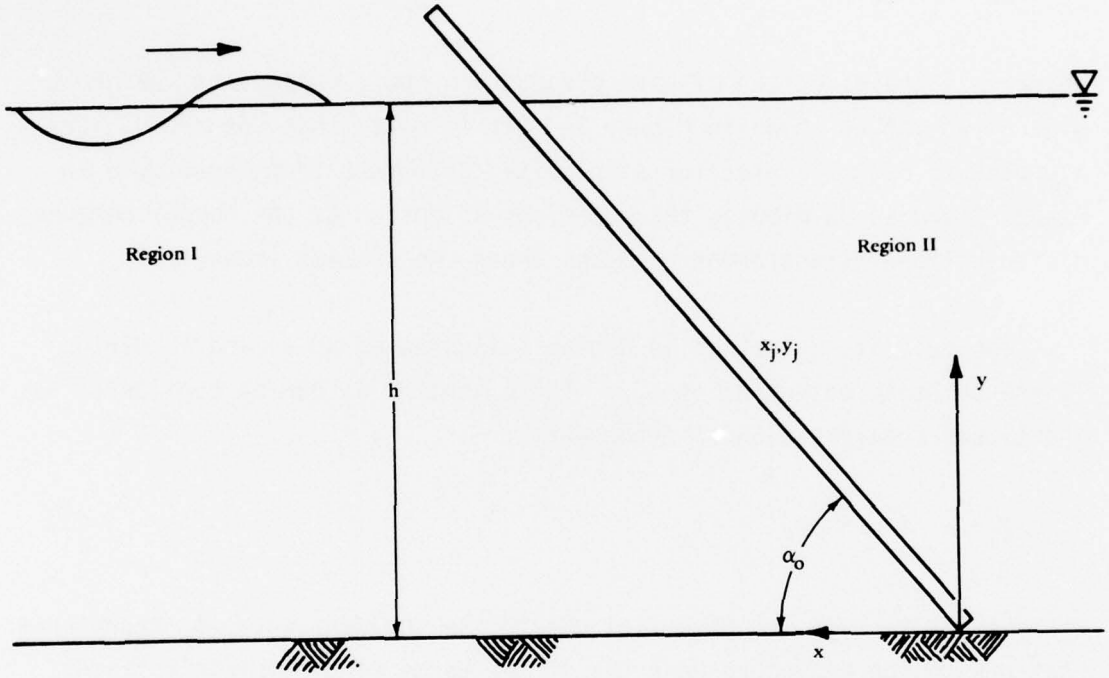

Figure 3. Definition sketch for evaluation of wave potential.

Therefore, the initial problem to be formulated relates to the waves generated from a hinged inclined-plate wave generator. In that case the velocity (and/or displacement) of the plate as a function of time is given and the amplitude of the waves in Region I or Region II is to be determined. This problem is exactly analogous to determining the scattered wave potential ϕ_s in the problem described by Eq. 2. Following the coordinate system described in Figure 3, the boundary conditions to be satisfied are:

$$\frac{\partial \phi_s}{\partial n} = 0 \qquad \text{on the bottom, } y = 0 \tag{3a}$$

$$\frac{\partial \phi_s}{\partial n} = f(x,y) \qquad \text{on the surface of the inclined plate (the n-direction is normal to the plate)} \tag{3b}$$

$$\frac{\partial \phi_s}{\partial y} = \frac{\sigma^2}{g} \phi_s \qquad \text{on the free surface, } y = h \tag{3c}$$

$$\frac{\partial \phi_s}{\partial x} \cong i\, k\, \phi_s \qquad \text{at } x = x_0\text{, to approximately represent the radiation condition} \tag{3d}$$

Since the region cannot be represented by a separable coordinate system, a solution to Eq. 1 can best be sought using an integral equation technique with:

$$\phi_s(\vec{x}) = \frac{1}{2\pi} \int_C \left[\ln\left(\frac{1}{r}\right) \frac{\partial \phi_s}{\partial n} - \phi_s \frac{\partial}{\partial n} \ln\left(\frac{1}{r}\right) \right] ds \tag{4}$$

If the field point, $\vec{x}$, approaches the boundary point $\vec{x}_j$, Eq. 4 can be written as:

$$\phi_s(\vec{x}_j) = \frac{1}{\pi} \int_C \left[\phi_s \frac{\partial}{\partial n} (\ln r) - \ln r \frac{\partial \phi_s}{\partial n} \right] ds \tag{5}$$

For solution, Eq. 5 can be approximated by a matrix equation with the mixed boundary conditions substituted into the matrix equation. The approximate solution for the potential $\phi_s(\vec{x}_j)$ can be expressed as:

$$\phi_s(\vec{x}_j) = M\, f \tag{6}$$

where M is an N x N matrix and N is the number of discrete elements into which the boundary is divided and f is a vector with non-zero value only on the plate; f represents the normal velocity of the plate. In this manner a solution for the velocity potential is obtained and from this the wave amplitude is determined.

The solution to this problem will be presented and compared to experiments in a later section. This becomes an extremely important element of the solution of the moored barge motions and mooring forces after connecting, with proper phase, the other elements of the solution ϕ_i and ϕ_r, since the final potential determines the pressure distribution around the plate and, hence, defines the forcing function.

4. The Dynamics of the Moored Body

To develop the equation of motion of the moored barge, it is necessary to determine first two restoring forces: the change in the buoyancy and the elastic restraint associated with the mooring lines. These restoring forces are then incorporated in the full equations of motion. With reference to Figure 4, due to the motion of the center of gravity a change in buoyancy is developed which acts as either a positive or a negative restoring force depending on the direction of the motion of the body. For the motion shown in Figure 4 in the x-direction, the y-direction, and the pitch-direction, ψ, there is a reduction in buoyancy represented by the shaded area $\overline{pqrs}$. Due to the motion, the point labelled "a" has moved to position "r" and that labelled "b" has moved to position "q". The equations which describe this change using the notation of Figure 4 are presented in Plate 1 where the area of $\overline{pqrs}$ denoted as A is shown to be a function of the coordinates of translation and rotation of the body. The moment associated with this change in buoyancy is presented in Plate 2. Thus, the buoyancy force and the associated moment give rise to an interaction among the equations of motion.

The restraining force which is associated with a mooring chain which depends primarily upon the unit weight for resistance to small motions has been developed, and it is quite complicated and is not presented here. The restraint discussed here is an elastic mooring line where the developed force is of the form: $T = C(\Delta s/s)^m$ (where $\Delta s/s$ is the strain and C and m are constants which depend on the type of line). The configuration used in considering the elastic mooring line is shown in Figure 5. The distance $\overline{OA}$ is defined as s, the length of the mooring line when it just becomes taut. When point A moves to A' the mooring line is stretched; the distance $\overline{OA'}$ becomes equal to $(s + \Delta s)$. To define the tension in the mooring line it is necessary to determine the strain $\Delta s/s$ which is described by the equations shown in Plate 3. The tension in the mooring line, T, can be related to the tension at breaking

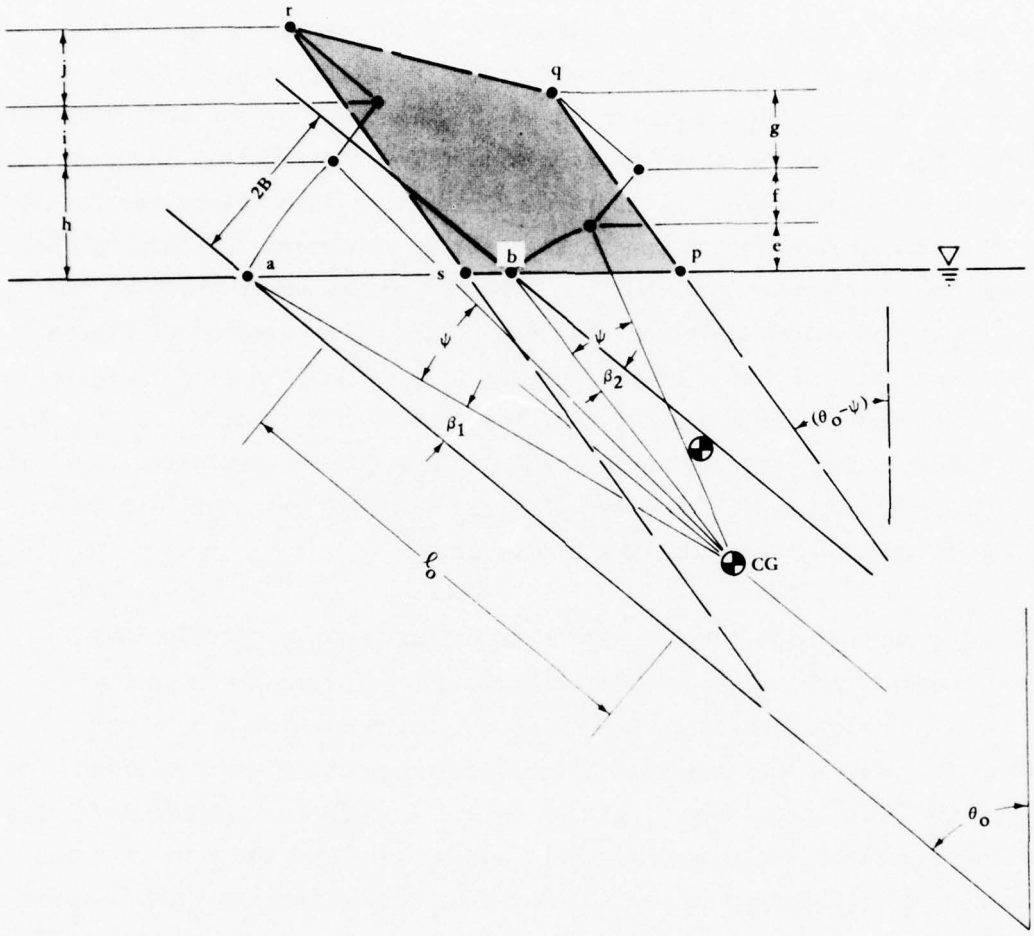

Figure 4. Definition sketch for the change in buoyancy.

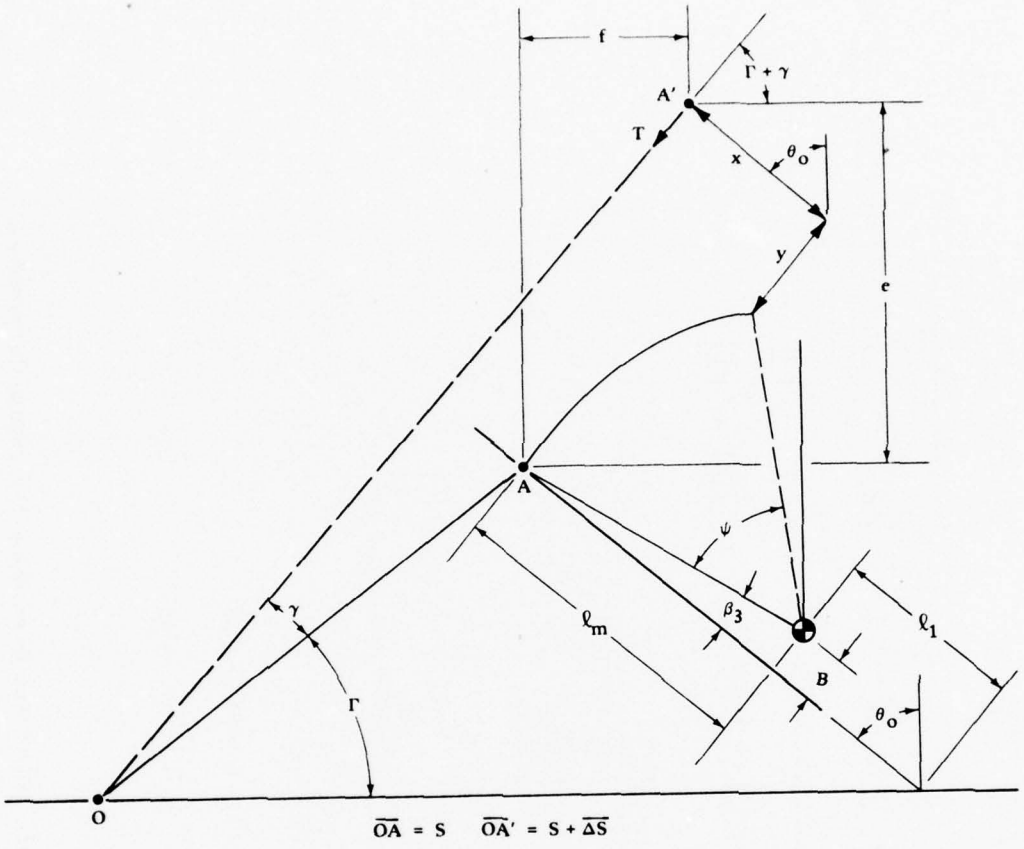

Figure 5. Definition sketch for mooring line restraint.

AREA pqrs $\equiv$ A

$$A = B\left[\frac{e + f + g + h + i + j}{\cos(\theta_o - \psi)}\right]$$

$$A = \frac{2B^2}{\cos(\theta_o - \psi)}\left\{\frac{y}{B}\sin\theta_o + \frac{x}{B}\cos\theta_o + \left[\sqrt{\left(\frac{\ell_o}{B} + \tan\theta_o\right)^2 + 1}\,\sin\left(\theta_o - \beta_2 - \frac{\psi}{2}\right)\sin\frac{\psi}{2}\right]\right.$$

$$\left. + \left[\sqrt{\left(\frac{\ell_o}{B} - \tan\theta_o\right)^2 + 1}\,\sin\left(\theta_o + \beta_1 - \frac{\psi}{2}\right)\sin\frac{\psi}{2}\right]\right\}$$

where: $\beta_1 = \sin^{-1}\left[\frac{1}{\sqrt{\left(\frac{\ell_o}{B} + \tan\theta_o\right)^2 + 1}}\right]$

$$\beta_2 = \sin^{-1}\left[\frac{1}{\sqrt{\left(\frac{\ell_o}{B} - \tan\theta_o\right)^2 + 1}}\right]$$

CHANGE IN BUOYANCY

x-Direction $\quad -\gamma_f A\cos(\theta_o - \psi)$

y-Direction $\quad -\gamma_f A\sin(\theta_o - \psi)$

Plate 1. Equations describing the change in buoyancy.

$$M_B = \gamma_f(\ell_1 + \ell_o)\ 2\ B\ w\ \ell_B \sin(\theta_o - \psi) - \gamma_f\ \ell_B\ w\ 2\ B^2 \tan(\theta_o - \psi)\left[\frac{y}{B}\sin\theta_o + \frac{x}{B}\cos\theta_o + \frac{\sin\left(\theta_o - \beta_2 - \frac{\psi}{2}\right)\sin\frac{\psi}{2}}{\sin\beta_1} + \frac{\sin\left(\theta_o + \beta_1 - \frac{\psi}{2}\right)\sin\frac{\psi}{2}}{\sin\beta_2}\right]$$

For rectangular barge of beam w

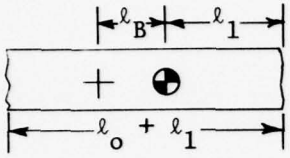

$$\ell_B = \frac{\ell_o - \ell_1}{2}$$

After movement of barge

$$\ell_B = \frac{1}{2}(\ell_o - \ell_1) - \frac{1}{4}\left(\frac{A}{4\ B}\right)$$

Plate 2. Equations describing the moment introduced due to the change in buoyancy.

$$e = \sqrt{B^2 + \ell_m^2}\left[\cos(\theta_o + \beta_3 - \psi) - \cos(\theta_o + \beta_3)\right] + y \sin\theta_o + x \cos\theta_o$$

$$\tan\beta_3 = \frac{B}{\ell_m}$$

$$f = \sqrt{B^2 + \ell_m^2}\left[\sin(\theta_o + \beta_3) - \sin(\theta_o + \beta_3 - \psi)\right] + y \cos\theta_o + x \sin\theta_o$$

$$\frac{\Delta s}{s} = \left\{\left[\sin\Gamma + \frac{\ell_m}{s}\sqrt{\frac{B^2}{\ell_m^2} + 1}\;\; 2\sin\left(\theta_o + \beta_3 - \frac{\psi}{2}\right)\sin\frac{\psi}{2} + y\sin\theta_o + x\cos\theta_o\right]^2\right.$$

$$\left. + \left[\cos\Gamma + \frac{\ell_m}{s}\sqrt{\frac{B^2}{\ell_m^2} + 1}\;\; 2\cos\left(\theta_o + \beta_3 - \frac{\psi}{2}\right)\sin\frac{\psi}{2} + y\cos\theta_o + x\sin\theta_o\right]^2\right\}^{1/2} - 1$$

$$\frac{T}{T_{BRK}} = C\left[\frac{\Delta s}{s}\right]^m$$

$$\sin(\Gamma + \gamma) = \frac{\frac{e}{s} + \sin\Gamma}{1 + \frac{\Delta s}{s}}$$

Plate 3. The restoring force for an elastic line.

by the expression shown in Plate 3; thus, once $\Delta s/s$ is defined the tension also can be determined knowing the characteristics of the mooring lines, defined by the constant C and the exponent m. (These coefficients are available for a number of synthetic-fiber lines.) It is important to observe that an initial tension may be put in the lines; hence, this is included also in Δs. The actual mooring lines have restoring force-displacement functions which are more complicated than this simple power law. Using actual data a polynomial will be fitted to the curve to obtain a solution.

With the restoring forces defined in terms of the motion of the barge, the equations of motion for this body can be presented following the notation of Figure 2. The equations of motion in the x-direction (surge), y-direction (heave), and ψ-direction (pitch) are presented in Plate 4.

Several important aspects of the equations of motion should be noted. It is sufficient to discuss the equation of motion in the x-direction since those terms in the y-direction and ψ-direction are analogous. On the left-hand side of the equation which describes motion in the x-direction is the mass of the barge times the acceleration in the x-direction which must be balanced on the right-hand side by the summation of all forces acting on the body. The first term on the right-hand side is simply the effect of the weight of the barge. The second term contains the effect of the buoyancy and the change in buoyancy (A); the latter, from Plate 1, is a function of the motion of the barge in the three coordinate directions. Thus, the second term on the right demonstrates one form of interaction among motions in the x, y and ψ directions. Of course, the angle ψ appears in all of the force terms on the right-hand side, showing the dependence of the acceleration in the x-direction on the pitch. The third term on the right relates the stress in the mooring line to the strain and is completely defined by the expressions presented in Plate 3. The fourth and fifth terms on the

right-hand side describe the normal force which acts on the bottom due to the submerged weight of the barge and the horizontal force associated with friction. (If initial tension is put in the mooring line this increases these terms.) The last term on the right-hand side is the forcing function, i.e., the integrated pressure force acting in the x-direction. This term is obtained, as shown, from the time derivative of the velocity potential obtained for Regions I and II. Thus, the motion in the x-direction is directly related to the solution for the velocity potential in those regions. It has been shown in Section 3, for the configuration described, the equation of motion is fully defined in terms of the incident wave amplitude. The equations of Plate 4 are programmed for solution on a digital computer following a time stepping method using available algorithms for solving a set of ordinary differential equations.

x-DIRECTION

$$m\ddot{x} = -W_s \cos(\theta_o - \psi) + \gamma_f w B\left[2(\ell_1+\ell_o) - \frac{A}{B}\right]\cos(\theta_o - \psi) + T_{BRK} C \left(\frac{\Delta s}{s}\right)^m \sin(\theta_o - \psi - \Gamma - \gamma)$$

$$+ N_N[\cos(\theta_o-\psi) + f_* \sin(\theta_o-\psi)] + \int_s p_x w\, ds$$

where: $p_x = \int_s \rho \left(\frac{\partial \phi}{\partial t}\right)_x ds$ — x-direction component of pressure around body

f_* = coefficient of friction with bottom

A = area associated with change in buoyancy. ds = elemental surface area

$m = W_s/g$

y-DIRECTION

$$m\ddot{y} = -W_s \sin(\theta_o - \psi) + \gamma_f w B\left[2(\ell_1+\ell_o) - \frac{A}{B}\right]\sin(\theta_o - \psi) - T_{BRK} C \left(\frac{\Delta s}{s}\right)^m \cos(\theta_o - \psi - \Gamma - \gamma)$$

$$+ N_N[\sin(\theta_o-\psi) - f_* \cos(\theta_o-\psi)] + \int_s p_y w\, ds$$

ψ-DIRECTION

$$I\ddot{\psi} = 2\gamma_f w B \ell_B(\ell_1+\ell_o)\sin(\theta_o-\psi) - 2\gamma_f w \ell_B B^2 \tan(\theta_o-\psi)\left\{\frac{y}{B}\sin\theta_o + \frac{x}{B}\cos\theta_o\right.$$

$$\left. + \frac{\sin\left(\theta_o-\beta_2-\frac{\psi}{2}\right)\sin\frac{\psi}{2}}{\sin\beta_1} + \frac{\sin\left(\theta_o+\beta_1-\frac{\psi}{2}\right)\sin\frac{\psi}{2}}{\sin\beta_2}\right\} - T_{BRK} C \left(\frac{\Delta s}{s}\right)^m \ell_m \cos(\theta_o - \psi - \Gamma - \gamma)$$

$$- N_N \ell_1[\sin(\theta_o-\psi) + f_* \cos(\theta_o-\psi)] + \int p_y w\, x\, ds$$

Plate 4. Equations of motion of moored body.

5. Presentation and Discussion of Results

Several different experiments have been conducted in an effort to investigate the validity of the analysis being conducted. An important early experiment consisted of investigating the waves generated by an inclined-plate wave generator hinged at the bottom of a wave tank. These experiments were conducted to compare to the formulation outlined in Section 3 concerning the scattered wave potential; this scattered wave corresponds to the wave created by an inclined-plate wave generator.

Experiments were conducted in a wave tank which is 60 ft long, 33 in. wide, and 12 in. deep. The wave machine was located at one end of the tank and a rock covered beach was placed at the opposite end for purposes of wave dissipation. In the initial experiments the heights of waves generated by an inclined oscillating plate were compared to those generated by a vertical plate, each hinged at the bottom. An example of some of the results is presented in Figure 6 for the plate with an inclination of 21.8° to the horizontal and the vertical plate ($\alpha = 90°$), the nomenclature used is defined in the inset in the figure. The abscissa is the ratio of the depth to the wavelength (h/L) and the ordinate is the ratio of the height of the wave produced to the stroke of the generator (H/S).

Included in Figure 6 are theoretical curves for the vertical and for the inclined plate generators which compare fairly well with the experiments. For the vertical plate both the theory and the experiments show a monotonic increase in generated wave height with an increasing ratio of the depth-to-wavelength for a given generator stroke. However, for the inclined wave generator ($\alpha = 21.8°$) the characteristics of the generation process appear quite different. For $0 < h/L < 0.14$ the inclined generator is more efficient than a vertical generator whereas for depth ratios greater than 0.14 the converse is true. (Agreement with the theory is reasonably good for $h/L < 0.14$). Indeed, three-dimensional effects may enter in the experiments; as mentioned, the

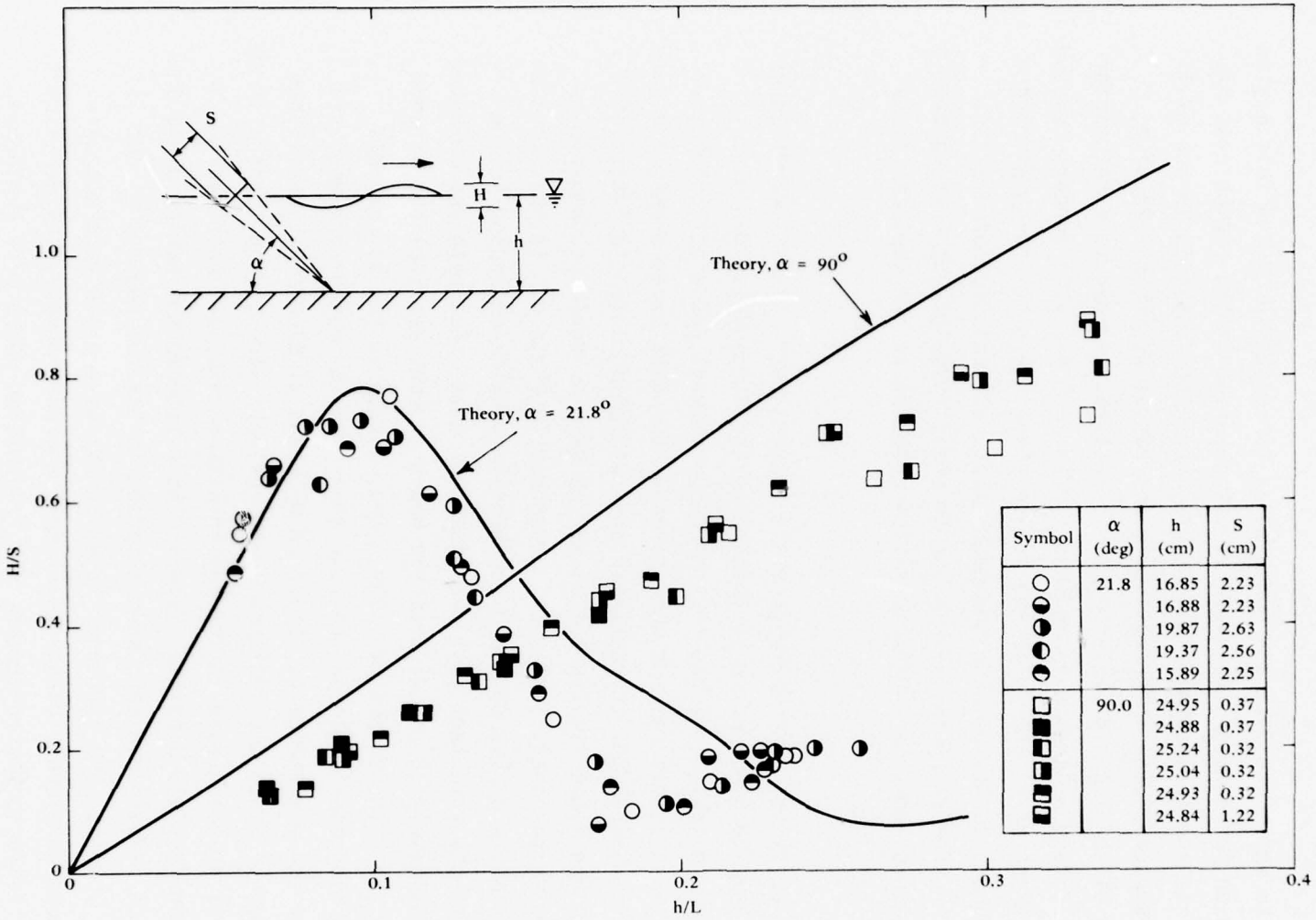

Figure 6. Wave generation characteristics of an inclined-plate generator; α = 21.8° and 90°.

theory to which the data are compared is two-dimensional and this may be the reason for some of the disagreement observed in the region near h/L = 0.2. If the horizontal distance from the hinge position to the still-water-surface-paddle intersection is defined as ℓ, for $\alpha = 21.8°$ a maximum of the ratio of wave height to generator stroke is attained for $\ell/L = 0.25$ and a minimum is reached for $\ell/L = 0.5$. This appears related to the trapping of energy in the region above the oscillating plate and this changes as the angle α changes. Thus, a local resonance effect which, in some respects, is similar to shelf resonance appears to modify the inclined generator characteristics compared to the vertical plate characteristics.

In addition to the wave-generator experiments, several other experiments have been conducted to understand the fundamental dynamics of motion of an inclined plate restrained by buoyant and elastic forces. Initially an effort was not made to model the AMMI barge shown in Figure 1, but to observe the transmission and reflection characteristics of a simple plate hinged to the bottom so the results could be compared to those using the analytical model presented in Plate 5. In the first set of experiments a plywood board one-half inch thick extending to the bottom of the wave tank just described was used; the depth was adjusted to approximately 15 cm, so that the board at rest was inclined between 18° and 19° with the bottom. The board, hinged at the bottom, was located near mid-length in the wave tank, and the waves were measured upstream and downstream of the board by means of electrical resistance wave gages. Since the inclined board reflects wave energy there will be a partial standing wave in the region between the wave machine and the plate and possibly a partial standing wave between the moving plate and the beach. Wave envelopes were obtained in the two regions (I and II) by slowly moving the carriages to which the wave gages were attached. From these envelopes, using small amplitude wave theory, the amplitudes of the incident, the reflected, and transmitted waves were evaluated.

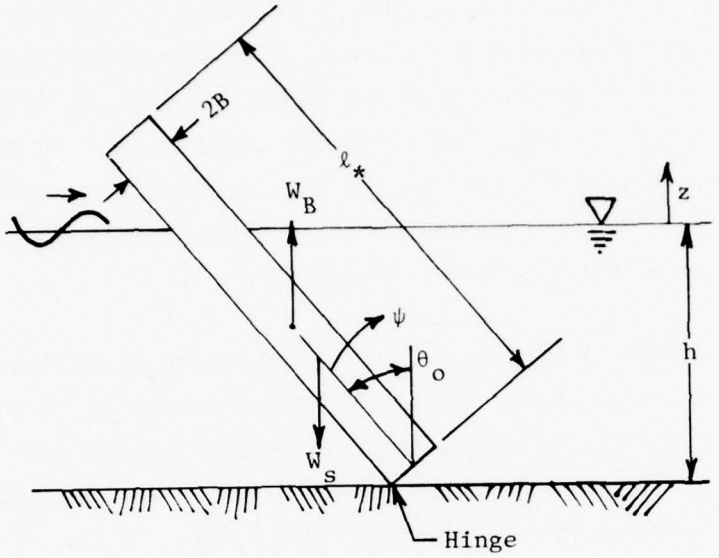

$$\ddot{\psi} = \frac{\gamma_f \, B \, w \, h^2}{I} \left[\frac{\sin(\theta_o - \psi)}{\cos^2(\theta_o - \psi)} \right] - \frac{W_s \, \ell_*}{2 \, I} \sin(\theta_o - \psi)$$

$$+ \frac{\rho \, w}{I \cos^2(\theta_o - \psi)} \int_o^{\frac{h}{\cos(\theta_o - \psi)}} \left[\frac{\partial \phi_1}{\partial t} - \frac{\partial \phi_2}{\partial t} \right]_{z, \theta_o, \psi} (h+z) dz$$

where: $I = \frac{W_s}{3 \, g} \left[\ell_*^2 + B^2 \right]$

$\left[\; \right]_{z, \theta_o, \psi}$ means bracketed term is function of z, θ_o, ψ

Plate 5. Equation of motion of a plate hinged at the bottom.

For the case of a plate extending to the bottom, two sets of experiments were conducted: with and without springs attached to the top of the board. For the experiments with the elastic restraint the springs were cantilever leaf springs consisting of two pieces of 2 in. by 1/32 in. aluminum plate. Thus, the restoring force was composed of both an elastic restoring force due to the springs and the restoring force due to changes in buoyancy. For the experiments without the springs the restoring force was due solely to changes in buoyancy.

In Figure 7 the change in the angle of the plate relative to the bottom is shown as a function of the force applied perpendicular to the plate. In this case the plate is restrained by the leaf springs just discussed. It is seen that this variation is nonlinear; the curve shown is an experimental curve best fit to the data.

If the spring is removed the restoring force becomes due to the change in buoyancy alone and the experimental and theoretical results for this arrangement are shown in Figure 8, where the angle of the plate with the bottom is plotted as a function of the applied force (normalized by one-half the weight of the plate). The experiments are in reasonable agreement with the analysis for the buoyancy restrained case at least for applied forces which are upward; again the nonlinearity of the restoring force is evident. The reason for the nonlinearity is that for a given angular displacement relative to the at-rest-position the change in buoyancy is different for increasing or decreasing angles. This effect is shown by the expressions presented in Plate 1 where the change in buoyancy is a nonlinear function of the angular change ψ.

The experimental results for these two restrained plates exposed to waves are shown in Figure 9 with the abscissa the ratio of the depth to the wave length and the ordinate the transmission coefficient, the reflection coefficient, and a quantity which is a function of energy loss in the system. The transmission coefficient is defined as the

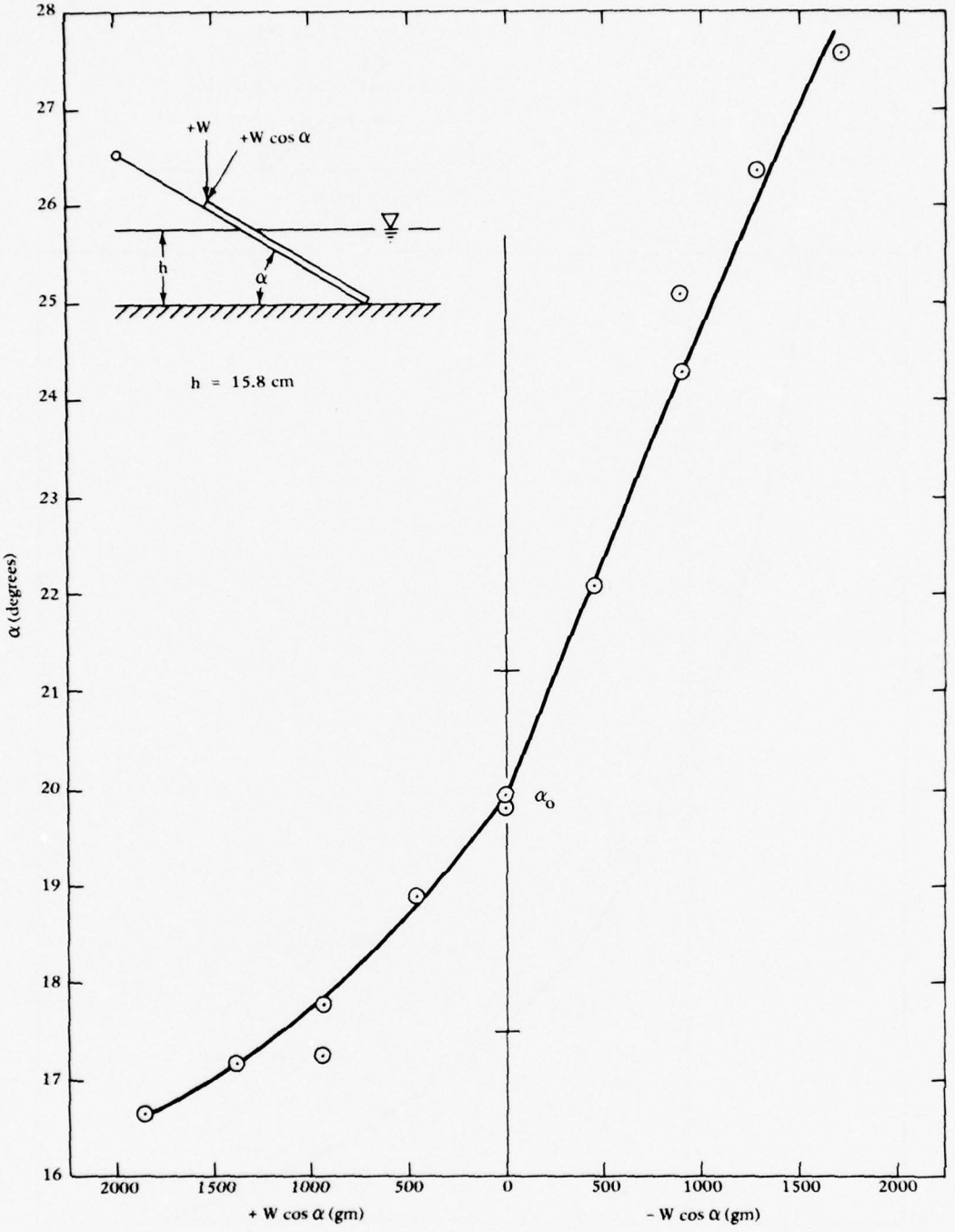

Figure 7. Deflection of board with elastic restraint under static load.

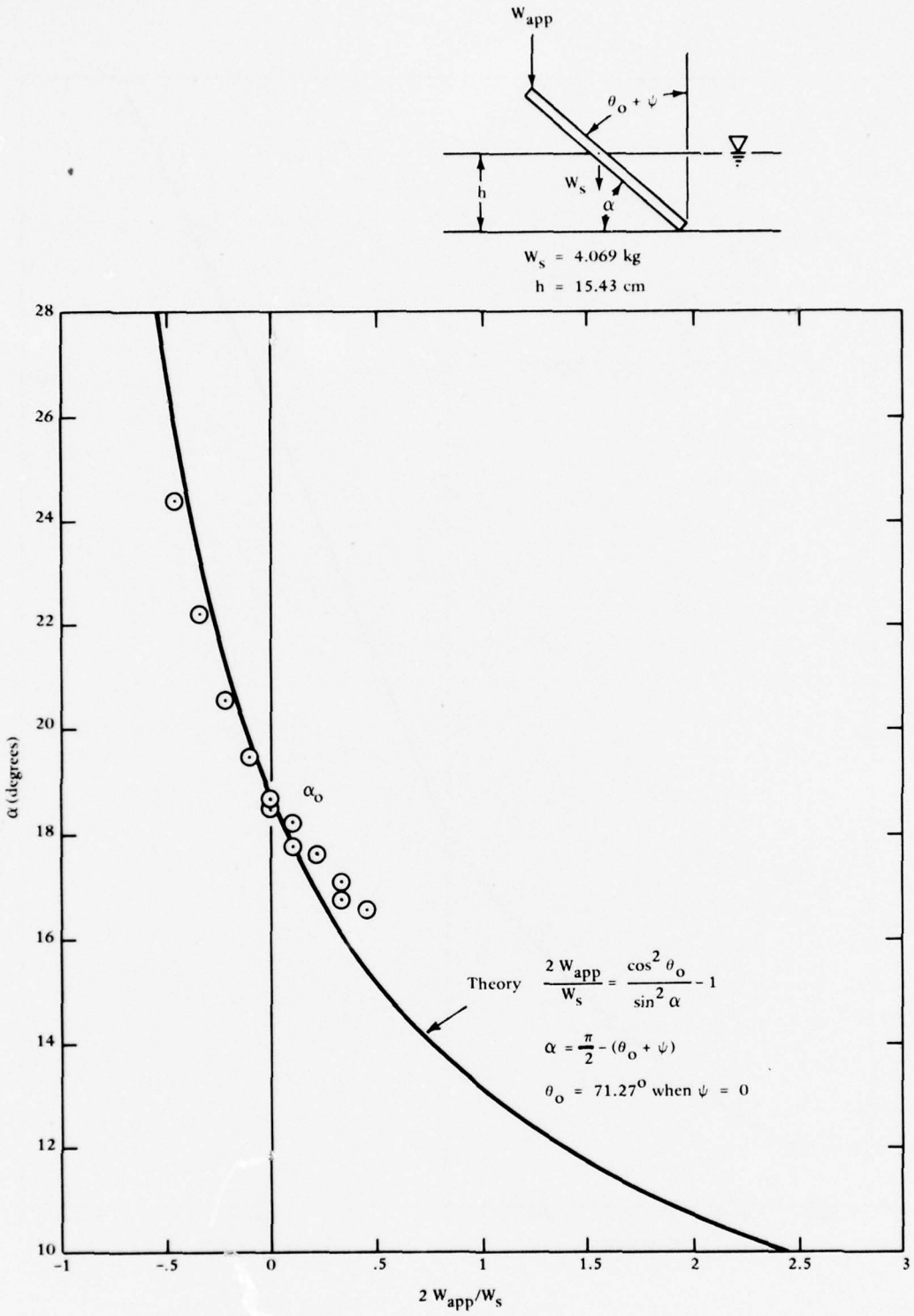

Figure 8. Deflection of unrestrained plate under static load.

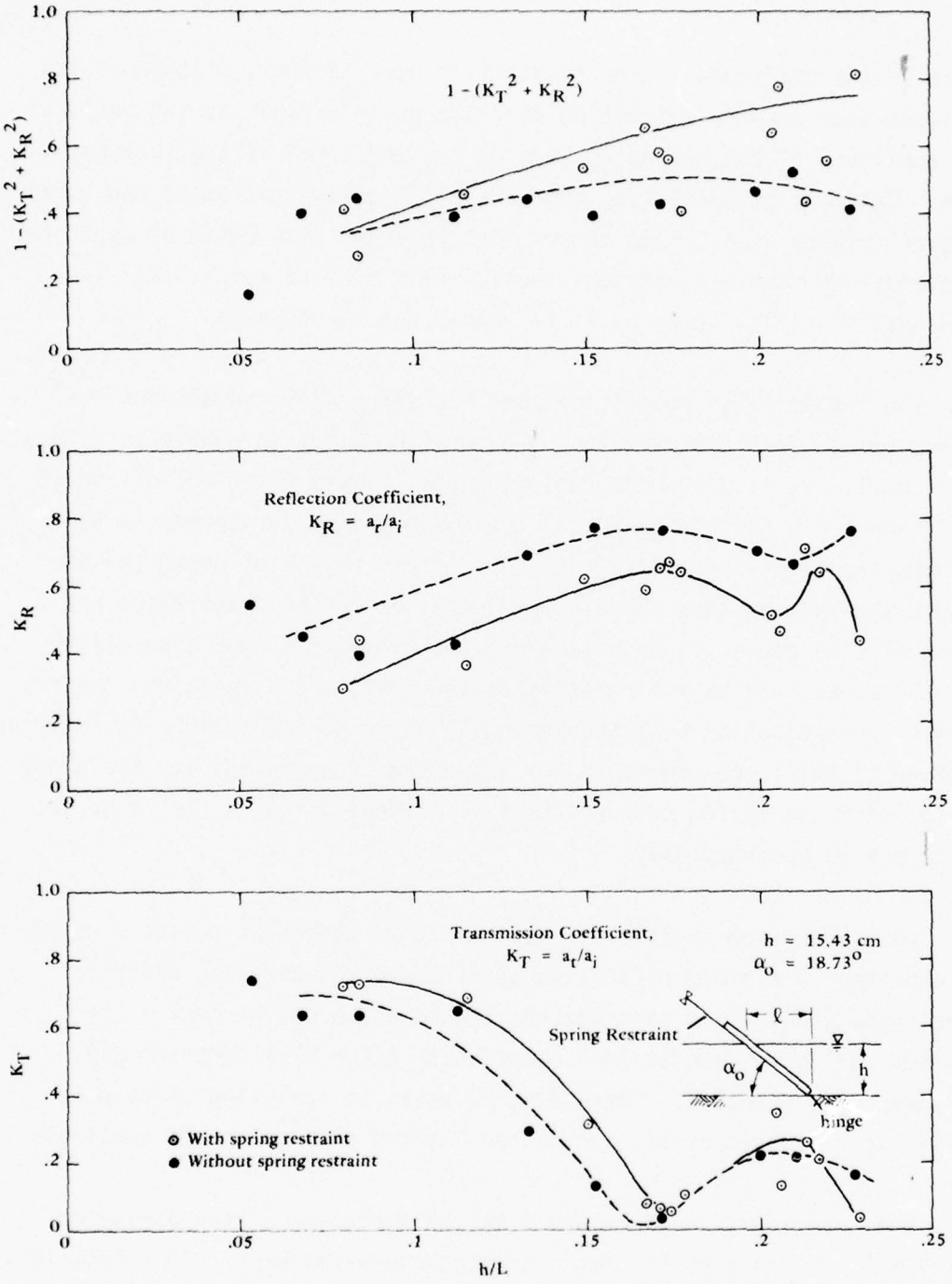

Figure 9. Characteristics of hinged plate with and without elastic restraint.

ratio of the amplitude of the transmitted wave to the amplitude of the incident wave and the reflection coefficient is defined as the ratio of the amplitude of the reflected wave to the amplitude of the incident wave. Data are presented for both the elastically restrained and unrestrained plates, i.e., with and without springs. The ratio of depth to wavelength for these experiments varies from 0.05 to about 0.22, i.e., from nearly shallow water waves to nearly deepwater waves.

The transmission coefficient for the cases with and without the spring varies from approximately 0.8 for long waves to nearly zero for $h/\ell = 0.17$. It is noted the ratio ℓ/L (see Figure 9 for definition of ℓ) is about 0.5 for the depth to wavelength which corresponds to this minimum transmission coefficient. For larger ratios of depth to wavelength the transmission coefficient increases and then decreases again. These effects appear to be related to the dynamics of the arrangement and the plate inclination relative to the bottom, and certainly deserve further investigation both theoretically and experimentally. An important feature of this arrangement is the increased transmission for the plate moored with the spring compared to that arrangement with the restoring force due to buoyancy only.

The reflection coefficient also exhibits important trends showing, as expected, a minimum reflection coefficient for the same depth-to-wavelength where there is a maximum transmission coefficient. The maximum reflection coefficient occurs near $h/L = 0.17$ ($\ell/L \cong 0.25$) followed by a decrease. (Care must be taken in analyzing certain of these experimental results due to the limited data which are available.)

The upper portion of Figure 9 is the variation of the parameter $[1 - (K_T^2 + K_R^2)]$ with the ratio of depth-to-wavelength. In effect this parameter is the difference between the incident wave energy flux and the energy flux which radiates in both directions from the hinged plate.

Hence, it represents the rate of energy dissipation due to viscous and mechanical effects. This portion of Figure 9 shows more power is required for motion of the hinged plate restrained by springs than for the system without springs for a given h/L; this is reasonable. This variation is in agreement with the variation of the transmission and reflection coefficients for the two cases.

It should be mentioned that these two models were crude since the investigation of certain dynamic and geometric effects were of main interest and the details of the actual barge were not considered as important as they would be in an hydraulic model of the actual barge. Nevertheless, one feature of the models should be noted. The hinges at the bottom for these experiments consisted of several brass "door hinges" which exhibited more friction than was desirable. Hence, although the two models could be compared to each other, these cannot be compared to the results of an accurate hydraulic model. (In fact for other experiments conducted, which will be discussed presently, the hinges were modified to significantly reduce the effects of friction.)

For comparison the dimensions of the prototype which were represented by the plate in these experiments are determined. Based on a prototype depth of 30 ft, this model had a length scale of 1/59.3, 1 foot in the model representing 59.3 ft in the prototype. Therefore, the prototype dimensions become: length = 118.2 ft, draft (2B) = 2.47 ft, and weight 160 tons for a beam of 28 ft; the model actually corresponded to a prototype with a beam of 163 ft since it was the width of the wave tank. This compares to the AMMI barge which has a length of 90 ft, a beam of 28 ft, a draft of 5 ft, and a weight of 50 tons. (If the length used were the same as the prototype, the weight would be 122 tons; if the prototype barge were flooded for 16 ft of length the weights would be comparable. The apparent large discrepancy in weight is due to the greater density of the model compared to the prototype barge.) Even with these differences, certain dynamic effects shown by the model are

important; the reason for conducting these particular experiments should be emphasized again. These experiments were conducted to form a base for checking the analytical model described in Plate 5 and to demonstrate certain dynamic effects and were not conducted considering the plate as an exact model of the actual barge.

Another group of experiments was conducted with a plate hinged at the bottom. In these, the hinge was materially improved from that used previously and consisted of two mating "eyes", one at 90° to the other with enough clearance between them so the connection could be considered almost "frictionless". This hinge allowed legs to be placed on the inclined plate so the arrangement could be hinged at the bottom and yet have a clearance between the bottom of the plate and the bottom of the tank. Thus, the situation could be modeled where the inclined plate was rigidly attached to legs hinged at the bottom. These experiments were conducted without elastic restraint so the only restoring force consisted of changes in buoyancy. The lengths of the different plates were adjusted so that the same initial slope (an angle to the bottom of 18.4°) was realized for the four cases tested: blockage ratios (a/h) of 1, 0.7. 0.5, and 0.27.

The results are shown in Figure 10 for the transmission coefficient, the reflection coefficient, and the "loss" parameter as a function of the product of wave number times the blockage length a, where the wave number is defined as $2\pi/L$ with L the wave length. (The nomenclature used is shown in the inset in the figure.)

Giving attention first to the lower part of the figure where the transmission coefficient is shown, for each case the data generally separate as a function of the percent blockage. In each case the minimum transmission coefficient moves to smaller values of the product of wave number times the blockage distance as the percentage of blockage increases. This may be a dynamic effect associated with the particular case under consideration.

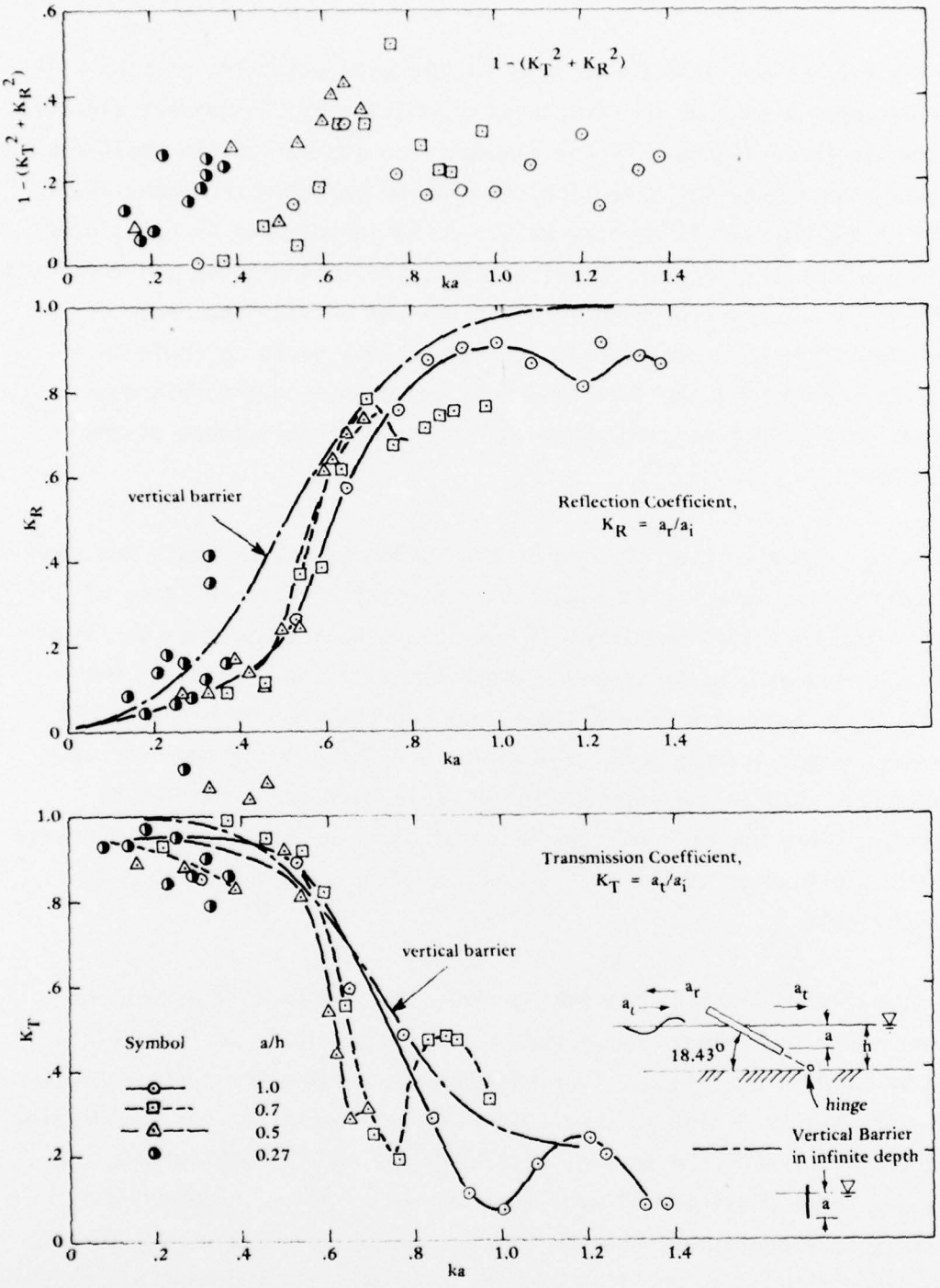

Figure 10. Characteristics of a hinged plate with and without clearance.

The reflection coefficient shown in the middle portion of Figure 10 also indicates a separation of data as a function of the percent blockage. Included in these figures are the transmission and reflection coefficients obtained from theory for a vertical barrier in an infinite depth; the length of the barrier is denoted as a. It is interesting to note, even though the theory is for an infinite depth, the transmission and reflection coefficients for corresponding values of ka are of the same order of magnitude as for the inclined moving plate. This tends to indicate a significant effect of the inclined plate on waves is due to blockage; however, more cannot be said about this feature at this stage of the development.

In the upper part of the figure the "loss" parameter which has been described in connection with Figure 9 is presented. For the case of a/h = 1, the value of this parameter is nearly one-half that shown in Figure 9 for corresponding depth to wave length ratios. One difference between the two experiments are the bottom hinges, so the results of Figure 10 indicate a significantly smaller loss for the "eye" hinge than for the "door" hinge used in the experiments whose results are presented in Figure 9. There may be some separation of data as a function of blockage; however, the scatter of the data is such that no attempt was made to delineate this.

A realistic model of the AMMI pontoon was constructed next to be tested in the laboratory and moored in a manner similar to that which would be used in the field. This was done as a guide for further analytical work and to assist in some initial design decisions for forthcoming field tests. There were several critical features in constructing the model and these consisted of modeling a barge which was geometrically similar to the prototype, had the correct weight when empty, the correct weight when flooded a specified amount, and the correct moment of inertia so that the motions of the model would correspond to those of the prototype. All of these features provided some significant design problems which were surmounted without considerable difficulty.

The model tests were to be conducted in a wave tank which is 3 ft wide, 3 ft deep, and 120 ft long. Therefore, considering the available ranges of the wave period and the depth in the laboratory, it was decided to operate at a prototype depth of 25 ft and a model scale of $L_r = 1/25$. To obtain similitude of the model, a model barge composed of a combination of plywood and styrofoam was used. The model consisted of one-quarter inch plywood faces with a 2 inch thick styrofoam block between; thus, this sandwich of plywood and styrofoam provided a thickness of approximately 2.5 inches (5.21 ft in the prototype). Therefore, the thickness is not modelled exactly; however, this approach resulted in a corresponding prototype weight (scaled for a 28 ft wide barge) of the barge of 95,168 lb, compared to the actual weight of 100,000 lb which was desired. This was considered to be a reasonably good model of the barge.

To weight the model to simulate the flooded barge (so that it would sink at the desired angle), it was necessary to develop a simple method of determining the amount of water necessary to flood the prototype barge to arrive at the desired angle. This evaluation can be made graphically using Figure 11. In Figure 11 the variation of one-half the flooded length of the barge is shown as a function of the resultant angle of the barge to the vertical and the water depth. Thus, the point shown for a 25 ft water depth which was to be modelled in the laboratory indicates that the barge should be filled to a length of about 72.45 ft in order to rest at an angle of 71.57° to the vertical (approximately one vertical on 3 horizontal). Without considering details of the interior barge construction, to meet this inclination, a weight of 649,138 lb of seawater would have to be added to the prototype. For a 3-ft wide model, this would correspond to an additional weight of 111.28 lb to achieve this angle which must be distributed with the center of gravity located, in the prototype, 36.22 ft from the sunken bow. This was achieved by adding two lead blocks to the model; each block weighed 55.64 lb and was located an appropriate distance from the center of gravity of the barge to provide the correct moment to sink the barge at

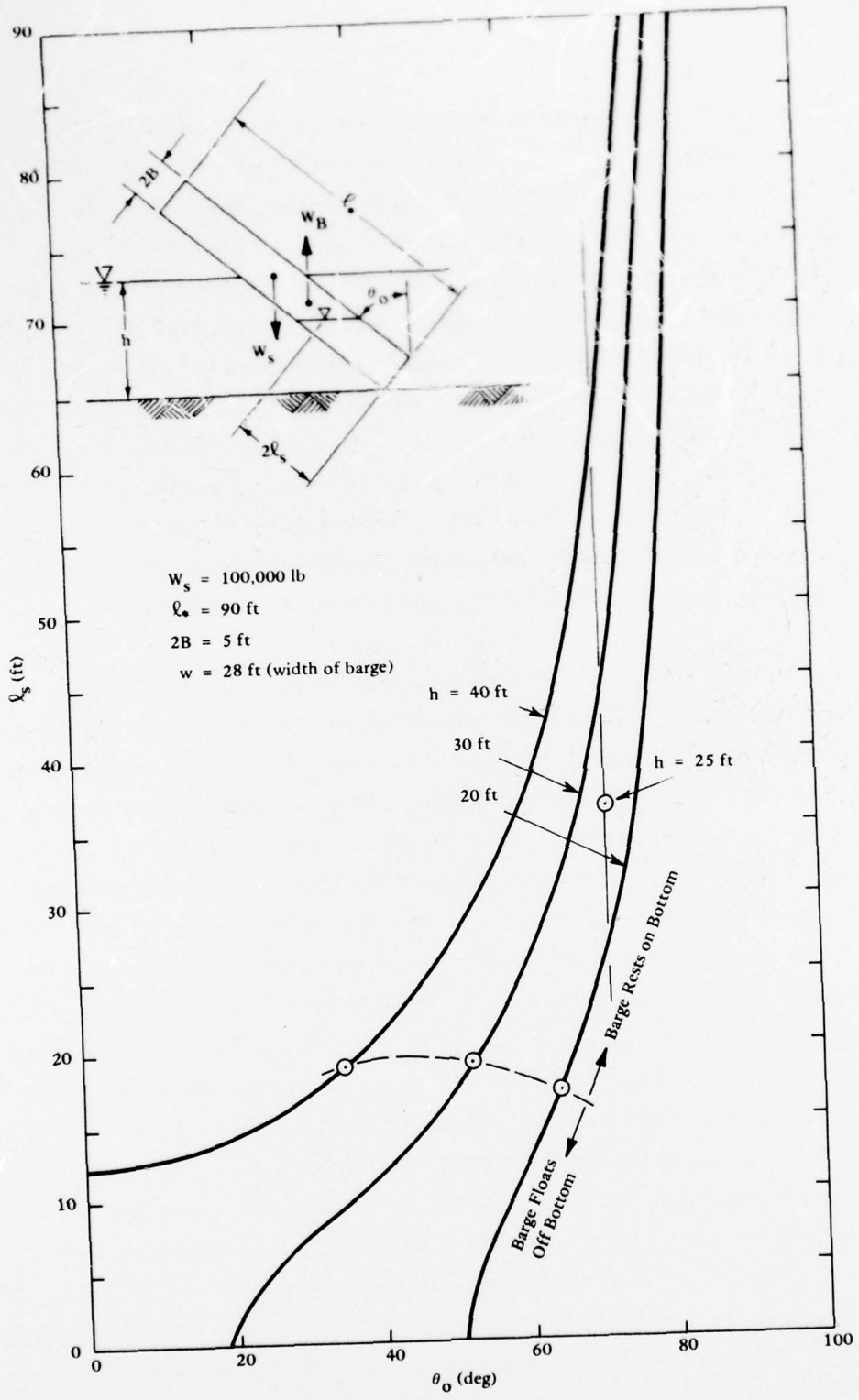

Figure 11. Equilibrium angle for unmoored, partly sunk AMMI barge; center of gravity at mid-length.

the desired angle and to provide the correct moment of inertia about the center of gravity. The blocks were cast to fit into a space cut into the styrofoam center of the model.

To compare how these conditions were met in the laboratory, Table 1 is presented, which shows the moment of inertia, in prototype dimensions, of the barge about its center of gravity and about the corner of the barge which rests on the bottom for three cases: the prototype barge, the present model which was just discussed, and the simple hinged plywood plate which was used in the early experiments. This table shows that for the AMMI model the moments of inertia, which must be modelled accurately, agree well with the prototype. It is important to observe that the hinged plate model, which was a simple plywood plate hinged to the bottom with an appropriate length to give the correct angle of inclination, has moments of inertia about the center of gravity and about the bottom hinge point which are approximately one-half that of the prototype. Thus, one would expect such an arrangement to exhibit more motion than the actual barge would under similar conditions if indeed it also were hinged at the bottom.

Table 1. Moment of inertia per unit width at prototype scale (lb sec^2 ft/ft).

Configuration	About the bottom contact point (J_o)	About the barge center of gravity (J_{cg})	J_o/J_{cg}
Prototype	1.53×10^6	4.37×10^5	3.49
Moored model	1.55×10^6	4.44×10^5	3.48
Hinged plate	0.86×10^6	2.15×10^5	4.0

The nonlinear mooring system was not modelled accurately for these experiments as decisions had not been made as to the mooring line configuration. A certain prototype mooring system was chosen composed of an artificial line material and this nonlinear force-deflection curve was subdivided into a series of linear segments. (For these experiments the model was moored linearly with one spring representing the first segment of the curve; future models will have the nonlinear mooring force modelled.) The plan for obtaining a nonlinear spring system in the model is to represent the actual force-displacement curve by a series of linear springs; thus, one problem was to develop the technique for making a spring with the desired spring constant. This is not a small task and considerable effort went into developing these techniques; the result was quite satisfactory. For example, for a desired spring constant of 910 lb/ft in the prototype, a model spring constant scaled up to prototype dimensions of 935 lb/ft was realized. The barge was then moored with this spring by using an inextensible line extending, at the desired angle, from the body to a pulley fastened to the bottom of the wave tank, then vertically through the water surface to one end of the spring; the other end of the spring was attached to a load cell. Thus, the spring was located above the water surface and the mooring force could be measured easily.

Experiments were conducted in the laboratory at a scale of 1/25 for a 25-ft depth of water for prototype wave periods which varied from 5 sec to 15 sec and for a prototype wave height of approximately 3 ft. Incident and transmitted waves were measured as well as the corresponding mooring force for two cases: one in which the body rested on the bottom, the other in which there was a gap of approximately 5.5% of the depth at the bottom. (It should be noted that including this gap changed the angle of the barge since the gap was obtained by adding legs to the barge; the angle was 73.88° to the vertical without legs and 75.04° with legs.) The barge was exposed to waves only for a limited time interval, which was determined as the time that it takes the first transmitted

wave to travel from the barge to a dissipating beach at the far end of the wave tank and back to the barge again. Since this time interval was less than the time for a "round-trip" of the incident wave, there were no reflected waves which excited the barge motion.

The results of these experiments are presented in Figure 12 where the lower half of the figure shows the variation of the transmission coefficient (defined as the transmitted wave height divided by the incident wave height) as a function of the product of the wave number and the depth; the upper portion of Figure 12 shows the mooring force as a function of the same abscissa. The mooring force is that which would be associated with a barge 28 ft wide; it should be noted that the barge used in the model really corresponded to one which was 75 ft wide due to the available flume width (3 ft).

Several important aspects of the wave transmission, reflection, and mooring forces are presented in Figure 12. In the lower portion of the figure it is seen that the moored model with the bow (or stern) resting on the bottom has a transmission coefficient varying from approximately 0.9 to nearly zero. When a small gap is introduced at the bottom, the transmission coefficient tends to be a little less for waves longer than about 7 sec and somewhat greater for waves shorter than about 7 sec. Both of these curves are below that presented for the hinged plate for waves with periods greater than 7 sec. This is perhaps reasonable, since the hinged plate had a smaller moment of inertia thus permitting larger movements for the same forcing function. Therefore, waves with substantially greater amplitude were transmitted.

The variation of the measured mooring force with kh is presented in the upper portion of Figure 12 for an incident wave height of approximately three feet. From observation this force is caused by the shoreward progression of the corner of the barge initially in contact with the bottom. This point moves with an oscillatory motion with this corner

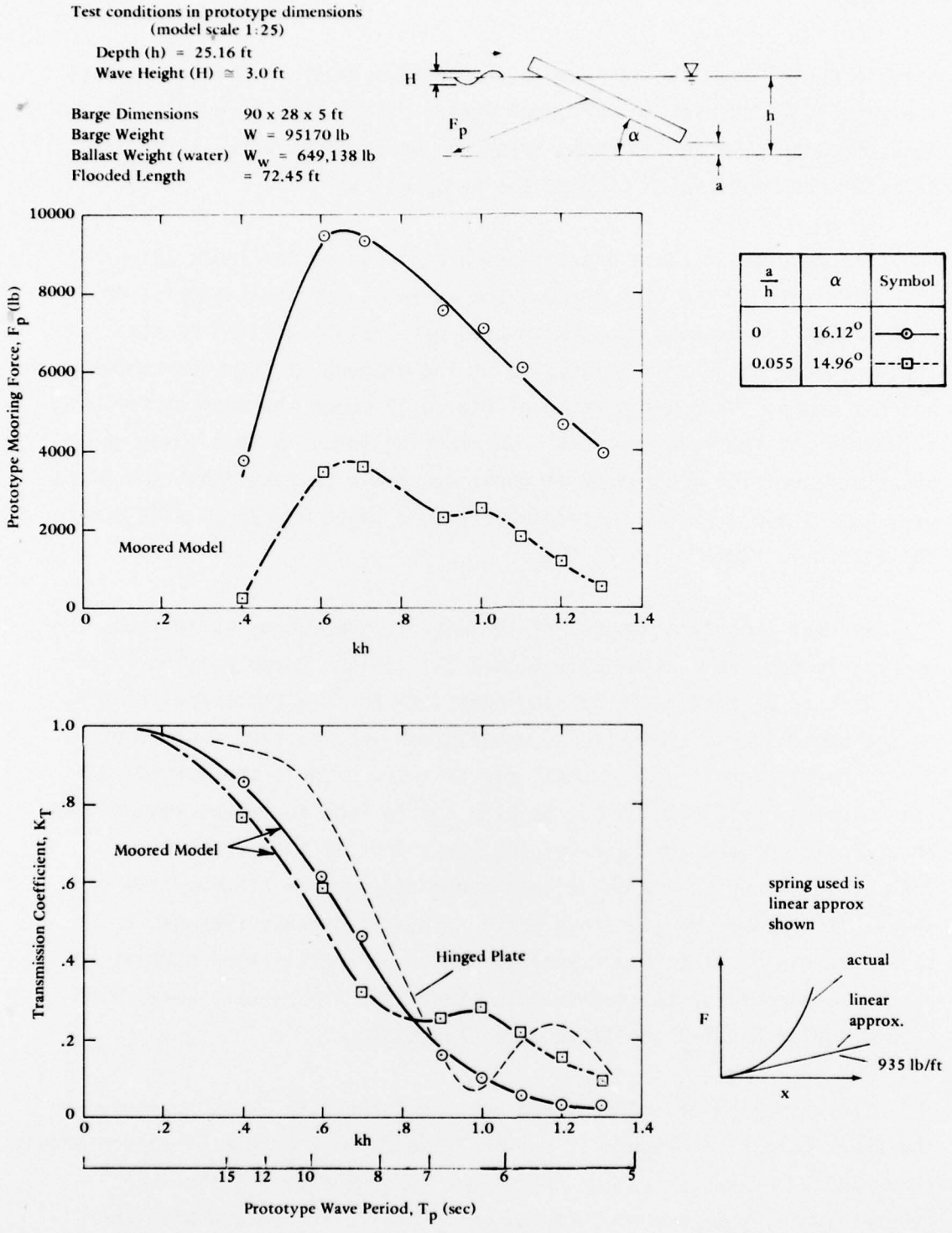

Figure 12. Transmission coefficient and maximum developed mooring force for moored barge.

lifting and moving shoreward, then returning to the bottom. The shoreward movement was limited by the developed mooring force; and a balance appeared to be reached between the applied and the restraining force. Thus, the force record had a mean trend which asymptotically approached a maximum value with a smaller amplitude periodic force superimposed.

Figure 12 shows, for the case of one end of the barge resting on the bottom, the maximum mooring force was approximately 10,000 lb for a wave period of about 10 sec and a transmission coefficient of approximately 0.6. In effect, the wave with this period caused the maximum shoreward motion of the barge. An extremely important and practically significant result of the experiments is that for a very small gap (about 5.5% of the depth) the mooring force is reduced by nearly a factor of three. Thus, the relief of pressure at the lower corner of the barge appears to reduce the shoreward progress of the barge for the same number of waves thereby reducing the mooring force. Of course, certain of these features will be investigated in much greater detail in future studies to more accurately define the mooring force as a function of the incident wave period and wave height.

6. Summary and Recommendations

In this report the important results of the investigation up to date have been presented and summarized. The major goals of the study were to investigate the dynamics of the semi-submerged AMMI barge with regard to the mooring line tensions and the barge motions. Concomitant were the wave reflection and transmission characteristics of the barge, to develop an analytical model to assist in the design of an optimum configuration for this type of mobile breakwater. Significant progress has been made toward achieving these goals.

The analytical problem can be divided into two parts: the evaluation of the wave potential in the regions to either side of the barge and the dynamics of the moored semi-submerged barge. The wave potential must be obtained to determine the pressure distribution acting on the barge. From this, the driving force and moment which result can be evaluated for use in the equations of motion. This is a difficult problem due to the inclination of the plate, but the problem is tractable and solutions obtained to date are confirmed by experiments which were conducted.

The equations of motion for the moored barge have been developed to define the motion and the mooring force. A time marching numerical solution is used for this part of the investigation starting with given incident wave conditions.

In addition to experiments relating to wave generation, there have been two other experimental models which have been studied in the laboratory. The first consisted simply of a hinged plate which was freely floating; thus, the restoring force was simply buoyancy. Experiments on the transmission and reflection characterisitcs of the plate have yielded interesting results for the system with a plate extending to the bottom and for cases where a gap has been left at the bottom. In all cases the

plate was hinged at the bottom and no attempt was made to exactly model either the weight or the moment of inertia of the AMMI barge. The primary reason for conducting these experiments was to compare with an analysis which would include both the scattered and reflective incident wave potential in the equations of motion of the plate.

Initial experiments were conducted with a moored model pontoon which accurately represented the prototype in terms of the geometry and the weight and moment of inertia. The length scale of this model was one foot in the model corresponding to 25 ft in the prototype. The mooring line used generated a linear mooring force which was softer than that which is contemplated for field use. Experiments were conducted to observe certain features of the movement of the barge where there was no physical connection of the barge to the bottom. The results were considered to be quite revealing and indicated that with a small gap at the bottom (of the order of 5 per cent of the depth) there was a significant reduction in mooring force without a great change in the transmissibility of wave energy. Several features of this study, which are discussed in the main text, indicate the importance of investigating in detail, both analytically and experimentally, the body moored in a nonlinear fashion with various gaps.

These exploratory experiments and analytical studies indicate that this type of system is indeed very promising as a mobile, partially floating breakwater to provide for a localized region of reduced wave activity. The extension of the initial concept of the partly submerged and moored pontoon to a pontoon which is placed at some distance from the bottom such that only partial blockage of the depth occurs, also appears to be an excellent idea in terms of wave attenuation and minimizing the mooring forces. This feature holds real promise in terms of partial reduction of transmitted wave energy allowing operation in deeper water.

To allow for proper engineering design in a general manner, more must be understood about the dynamics of the mooring of such structures, the associated mooring forces, and the resultant transmitted wave energy. At this time the basic dynamics of the system are appreciated if not completely understood, and additional analytical and experimental studies are considered both warranted and necessary. An analytical model can be developed which would be able to assist in defining the motions, wave transmission characteristics, and the mooring line forces associated with such a moored and partly sunk pontoon or barge. Of immediate need are additional experiments conducted with the modelled barge and the true nonlinear mooring restraint which is contemplated for the field. Such experiments would make a rational approach to the field experiments possible and provide data to compare to the results of field tests. With an understanding of the motions of such a system, the completion of the analysis is considered important so that the design of such a mobile breakwater can proceed in a more logical manner. With the proper analytical program, various mooring configurations could be explored and decisions made on mooring and motions for given wave conditions.

7. References

Gilbert, G., Thompson, D. M., and Brewer, A. J., "Design Curves for Regular and Random Wave Generators," Journal of Hydraulic Research, Volume 9, No. 2, 1971, pp. 163-196.

Patrick, D. A., "Model Study of Amphibious Breakwaters," Office of Naval Research, Series 3, Issue 332, Berkeley, CA, Oct 1951.

Ursell, F., Dean, R. G., and Yu, Y. S., "Forced Small Amplitude Water Waves: A Comparison of Theory and Experiment," M.I.T. Hydrodynamics Lab T.R. 29, 1958.